



Temperature Controls on the Erosion of Badland Slopes in the Nanxiong Basin, China

Zhi Chen^{1,2*}, Luobin Yan^{3*}, Hua Peng¹ and Hong Shi⁴

¹School of Geography and Planning, Sun Yat-sen University, Guangzhou, China, ²School of Geography and Planning, Nanning Normal University, Nanning, China, ³School of Geographical Sciences, Southwest University, Chongqing, China, ⁴School of Tourism and Historical Culture, Southwest Minzu University, Chengdu, China

OPEN ACCESS

Edited by:

Guobin Fu,
CSIRO Land and Water, Australia

Reviewed by:

Tao Gao,
Institute of Atmospheric Physics,
(CAS), China
Liuqin Chen,
East China University of Technology,
China

*Correspondence:

Zhi Chen
chenzhi0111@nnu.edu.cn
Luobin Yan
yanluobin@swu.edu.cn

Specialty section:

This article was submitted to
Hydrosphere,
a section of the journal
Frontiers in Earth Science

Received: 19 May 2021

Accepted: 06 July 2021

Published: 21 July 2021

Citation:

Chen Z, Yan L, Peng H and Shi H
(2021) Temperature Controls on the
Erosion of Badland Slopes in the
Nanxiong Basin, China.
Front. Earth Sci. 9:712134.
doi: 10.3389/feart.2021.712134

Understanding the relationships between environmental variables and erosion rates in badlands is vital for forecasting sediment yields. While the controlling role of rainfall on badland erosion rates has long been recognized, here we assess the relative influences of temperature and precipitation on slope erosion rates in the Nanxiong Basin, Southeast China. The volume of weathered and transported fragments was measured within a bounded plot at ten-day intervals between May 1, 2016, and April 30, 2017, and temperature and precipitation were continuously recorded. Mann-Kendall τ correlation, Granger causality, impulse response, and variance decomposition analyses were performed. The results show that Granger causality relationships exist between the ten-day mean temperature (TMT) and ten-day mean erosion rates (TER) and between the ten-day total precipitation (TTP) amount and the TER. Moreover, our findings indicate that TMT and TTP explained 14.6 and 12.61% of the variability in slope erosion rates, respectively, which indicates that temperature had at least the same influence on slope erosion than precipitation. In addition, because 22.5% of the measured erosion occurred during periods when there were no erosive rain events, the importance of small dry slides for removing rock fragments from these humid slopes is emphasized.

Keywords: badlands, erosion rates, granger causality test, M-K tau test, nanxiong basin

INTRODUCTION

Badlands are commonly defined as ‘intensely dissected natural landscapes where vegetation is sparse or absent and useless for agriculture (Bryan and Yair, 1982). Due to their high erosion rates, badlands are also viewed as degraded areas worldwide (Brandolini et al., 2017; Molina et al., 2009; Peng et al., 2015). Soft bedrock and a lack of vegetation both promote accelerated erosion in these landscapes that produce steep, highly dissected topography and the formation of gully networks and badlands (Fairbridge, 1968; Bocco, 1991). As a result, Badland areas have some of the highest erosion rates globally (Clarke and Rendell, 2010). Consequently, they are considered as ‘ideal field laboratories’ for studying landscape evolution, acting as miniature fluvial systems in which it is possible to directly observe hill slope-scale processes, interconnections, and resulting landforms (Bryan and Yair, 1982; Parsons and Abrahams, 1994; Campbell, 1997; Alexander et al., 2008; Dickie and Parsons, 2012; Yair et al., 2013).

Several factors and processes affect the development and dynamics of badlands, most notably lithology (Kasanin-Grubin and Bryan, 2007; Morenode las Heras and Gallart, 2016), climate (Bryan and Yair, 1982), and slope aspect (Nadal-Romero et al., 2007). Marked differences in badland slope morphology (Churchill, 1981) and species richness (Nadal-Romero et al., 2014) have been

recognized between aspects, and slope aspect can also be one of the most critical factors determining the intensity of physical weathering processes (Regüés et al., 2000). For a specific badland site, lithology and slope aspects are fixed over long temporal scales relative to climate. Thus, an important aspect of forecasting erosion rates in these landscapes is determining the influence of individual climatic factors.

The rate at which badland landforms develop is the subject of continued speculation (Clarke and Rendell, 2006). For example, erosion rates between 32 and 77 Mg ha yr⁻¹ in non-vegetated badlands have been recorded in the Bardenas Reales, southeast Spain (Desir and Marin, 2009), compared with rates of between 16 and 63 Mg ha yr⁻¹ in vegetated badlands in the Penedès region of Spain (Martínezcasasnovas et al., 2010). In the Guadalajara badlands of Spain, erosion rates of up to 114 Mg ha yr⁻¹ have been reported (Martín-Moreno et al., 2014).

Rainfall is an important driver of high erosion rates in badlands. For example, statistically significant relationships between sediment yield and the number of rainfall events have been reported (Cantón et al., 2001), which implies that wetting-drying cycles might have a more significant influence on weathering compared to the individual effects of heating and cooling cycles caused by temperature fluctuations (Cantón et al., 2001). Exceptions to this include badlands in Saudi Arabia, Kuwait, Qatar, and Yemen, where desert-like conditions prevail with substantial differences between day and night temperatures (Erguler and Shakoor, 2009). Erosion rates are assumed to be closely related to average annual precipitation (Bull and Kirkby, 2001), with the relationship between cumulative rainfall and cumulative erosion being particularly strong (Clarke and Rendell, 2006; Schumm, 1964). In addition, rain splash and creep caused by rainfall events can contribute to the detachment and transport of particles from slope face (Cantón et al., 2001). Thus, we hypothesized that in humid subtropical areas, erosion rates would be more strongly correlated with precipitation than temperature.

Although the role of temperature in the rapid weathering of badland materials has been studied (Yan et al., 2019), the impact of temperature on the erosion processes remains relatively understudied. Many existing studies on erosion rates in badlands have been undertaken on a yearly or decadal scale (Clarke and Rendell, 2006; Clarke and Rendell, 2010) and, as a result, the temperature is often averaged across an entire year. About methods, most previous studies have deployed erosion pins, which are considered an inaccurate means of monitoring short-term erosion rates and, therefore, have limited value in assessing the impacts of environmental variables. Thus, fine-scale erosion rate measurements are required to study the possible influences of temperature and predict future erosion rates to inform erosion-control measures (Cantón et al., 2001). Therefore, this study aimed to determine the relative contributions of temperature and rainfall to the erosion of badland slopes.

STUDY AREA

The Nanxiong Basin (24°33′–25°24′ N, 113°52′–114°45′ E), an ancient, Cretaceous faulted rift basin in the fold belt of the Nanling Mountains, is located in north Guangdong Province, southeast China. The basin has an elevation range of 48 to 1,421 m above sea level (Dogan and Aslan, 2017) and covers an area of 2,214 km² (Figure 1). The basin has a subtropical monsoon climate with long hot summers and short winters. According to the Nanxiong meteorological station (1956–2010), the mean annual temperature, precipitation, and potential evaporation rate are 19.6°C, 1,555.1 mm, and 1,678.7 mm, respectively (Yan et al., 2017). In addition, continuous successions of red fluvial-lacustrine clastics with a maximum thickness of more than 7 km are preserved in the basin (Ma et al., 2018).

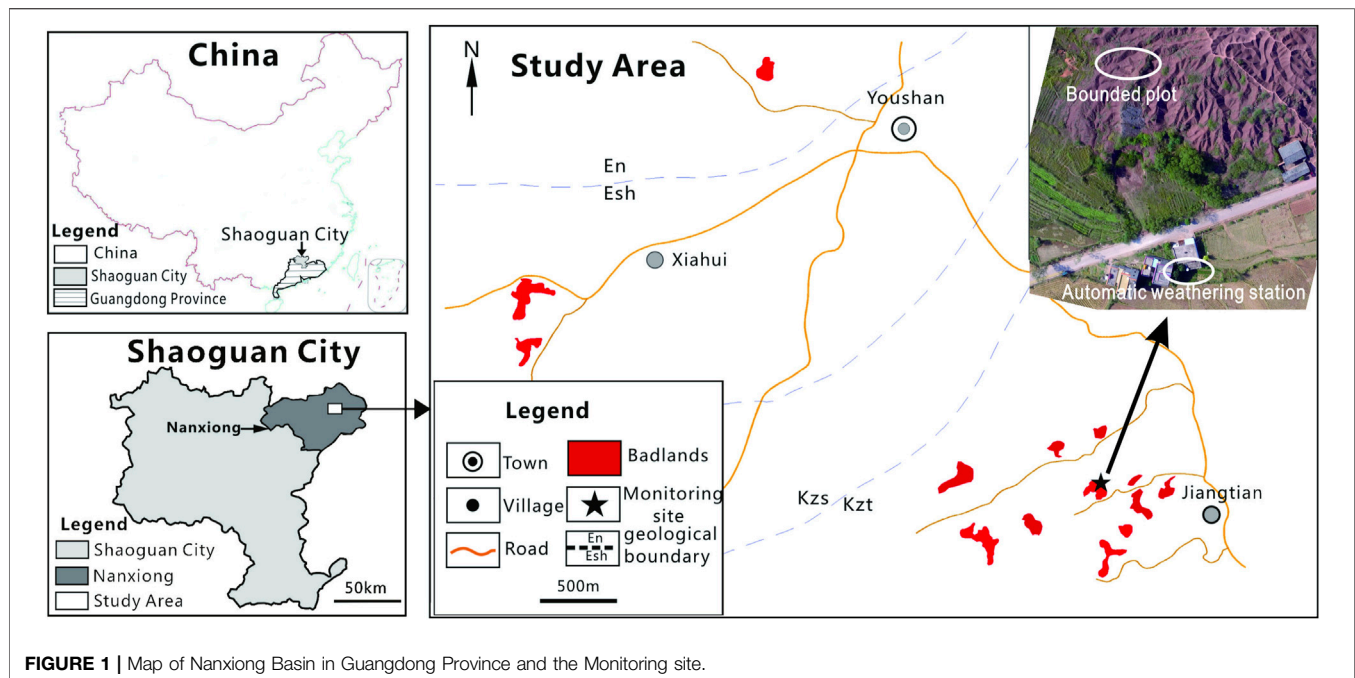
Visually spectacular badland landscapes are well developed over a homogeneous and monotonous series of calcareous silty mudstones and siltstones in the Nanxiong Basin (Figure 2). These are incised into continental purple mudstones from the Nongshan Formation (En) in Dahangkeng Village, the Shanghu Formation (Esh) in Huangtian Village, and the Zhutian formation (Kzt) in Jiangtian Village. Most studies conducted in this area have focused on the nature of the purple soils rather than erosion of the badland landscapes themselves (Jiang et al., 2015).

MATERIALS AND METHODS

Erosion Monitoring

To control for slope aspect, we established two bounded plots (1.6 × 2 m) on two opposite slopes oriented in an E–W direction (Figure 3). Weathered fragments (detached material) that had been eroded and transported to the platforms at the foot of each slope were collected. The slopes were left untouched for 12 months. The upper part of each plot was open, and, in the lower part, the platform from which regolith was collected was bounded by a brick wall. Outlets to drain water in platforms were set in the walls and were covered with a filter screen to trap regolith. At approximately ten-day intervals, regolith fragments were collected from the bases of the slopes, dried in an oven for 24 h at 100°C, and their dry weight was recorded. Given the fixed area of the bounded plots and experimental time interval, time-series erosion rate datasets could be easily calculated.

Given the problems associated with observations over just one season (Regüés et al., 1995), fragments were collected across an entire year, between May 1, 2016, and April 30, 2017. Given the low amounts of Ca₂CO₃ in the rocks forming this area (Yan et al., 2019), the potential loss of material from the dissolution of calcareous material was not considered. Moreover, given the low relief of these badlands (with a topographic range of approximately 20 m), topography was not considered. Unfortunately, one of the bounded plots was vandalized 3 months into the monitoring period, and, as such, results for one plot are discussed here.



Rainfall and Temperature

An automatic weather station was installed 200 m away from the experimental plot, which was connected to an automatic data logger. Temperature and precipitation recordings were made at 10-min intervals over the 12 months of field monitoring.

Mann-Kendal τ Correlation Coefficient and Granger Causality

The Mann-Kendal (M-K) tau test is a nonparametric test that does not require data with a specified distribution. M-K τ correlation coefficients for the measured erosion rates and

environmental variables (temperature and rainfall) were calculated using MATLAB software. The Granger causality test is a statistical test used to determine whether one time series is useful for forecasting another (Granger, 1969), which has been widely used to study the dynamic relationships between economic time-series (Granger, 1988). Here, Granger causality tests were performed using Eviews software (version 11), which can be used for general statistical analysis and econometric analyses, such as cross-section and panel data analysis, and time-series estimation and forecasting. All of the variables used in our analyses are presented in **Table 1**.



FIGURE 3 | The environment of the study site and the instruments for monitoring of erosion rates. We chose a site where the gully bottom is not steep to construct a cement platform to collect regolith depletion.

RESULTS

Erosion Rates and Erosional Modulus

The mean erosion rate for the whole year, which was calculated as the weight of fragments collected at the base of the experimental slope during the study year divided by the plot area, was $140 \text{ Mg ha}^{-1} \text{ yr}^{-1}$. The highest erosion rate was logged during October 20th–30th, 2016, at $440 \text{ Mg ha}^{-1} \text{ yr}^{-1}$. Conversely, the lowest erosion rates recorded were $2.92 \text{ Mg ha}^{-1} \text{ yr}^{-1}$, $8.03 \text{ Mg ha}^{-1} \text{ yr}^{-1}$, and $4.02 \text{ Mg ha}^{-1} \text{ yr}^{-1}$, which occurred during January 1–11, January 11–20, and January 20–30, 2017, respectively (Figure 4).

August 2016 had the highest mean erosion rate at $313.58 \text{ Mg ha}^{-1} \text{ yr}^{-1}$ (calculated by dividing the sum erosion amount of each month and 12 months/year per area) (Figure 3). Conversely, the months with the lowest erosion rates were December, January,

and February, at $4.76 \text{ Mg ha}^{-1} \text{ yr}^{-1}$, $27.01 \text{ Mg ha}^{-1} \text{ yr}^{-1}$, and $35.66 \text{ Mg ha}^{-1} \text{ yr}^{-1}$.

Similar to most transport-limited slopes of badlands (Campbell and Honsaker, 1982), the badlands slope in Nanxiong Basin is covered with a thick layer of rock fragments, especially on the slope faces. As its slope is equal or close to the critical slope of fragments, even during periods without rain, weathered fragments were still found in the plot platform. For example, during September 13–21, 2016, and December 30, 2016, to January 11, 2017, there was a marked difference in erosion rates, at $195.64 \text{ Mg ha}^{-1} \text{ yr}^{-1}$ and $2.92 \text{ Mg ha}^{-1} \text{ yr}^{-1}$.

Given that not all rainfall events cause erosion of the regolith, the term ‘erosive rain’ can be applied to those rainfall events to initiate transport. A threshold for such events of 12.7 mm of total rainfall has been suggested by Wischmeier and Smith, (1978), while Jiang and Li (1988) suggest a lower value of 10 mm that is more applicable to badlands considering the presence of dry regolith, which is more vulnerable to erosion. During the year-long study, no erosive rainfall events ($>10 \text{ mm}$) were observed during several of the monitoring periods (Table 2). Without removing fragments caused by rain, the highest and lowest erosion rates were $195.64 \text{ Mg ha}^{-1} \text{ yr}^{-1}$ and $2.92 \text{ Mg ha}^{-1} \text{ yr}^{-1}$, respectively, representing a difference of 65 times. The erosion occurring during these ‘dry’ periods accounted for 22.5% of the total erosion amount.

Statistical Analysis

The correlation coefficient between monthly and ten-day erosion rates and various environmental variables shown in Table 1 was obtained by applying the M-K tau correlation. Strong correlations were observed between the environmental variables, including monthly mean temperature, monthly mean temperature of daily highest temperature, monthly mean temperature of daily lowest temperature, and monthly erosion rate. Most of the calculated correlations of the ten-day erosion rates with environmental variables were positive and statistically significant ($p \leq 0.01$) (Table 1). Based on these data, temperature appeared to significantly influence on erosion rates than rainfall during the study period.

Granger Causality Tests

Tried with different environmental variables, finally, ten-day mean temperature (TMT) and ten-day total precipitation (TTP) were selected to test the causality between variables. The results of

TABLE 1 | Nonlinear correlations for Monthly and Ten-day erosion rates and environmental variables.

Correlation coefficient	Monthly erosion rates	Correlation coefficient	Ten-day erosion rate
Monthly mean temperature	0.7878 ^a	Ten-day mean temperature	0.4476 ^a
Monthly total precipitation	0.3091	Ten-day total precipitation	0.4073 ^a
Number of rainfall events	0.4545	Ten-day number of rainfall events	0.4871 ^a
Total precipitation (only including rainfall events over 10 mm)	0.3273	Ten-day precipitation (only including each rainfall event over 10 mm)	0.4456 ^a
Monthly mean temperature of daily highest temperature	0.8182 ^a	Ten-day mean temperature of daily highest temperature	0.4839 ^a
Monthly mean temperature of daily lowest temperature	0.8364 ^a	Ten-day mean temperature of daily lowest temperature	0.5181 ^a
Monthly highest temperature	0.3273	Ten-day highest temperature	0.4839 ^a
Monthly mean temperature difference	0.1455	Ten-day mean temperature difference	0.0121

^aStatistically significant where $p < 0.01$.

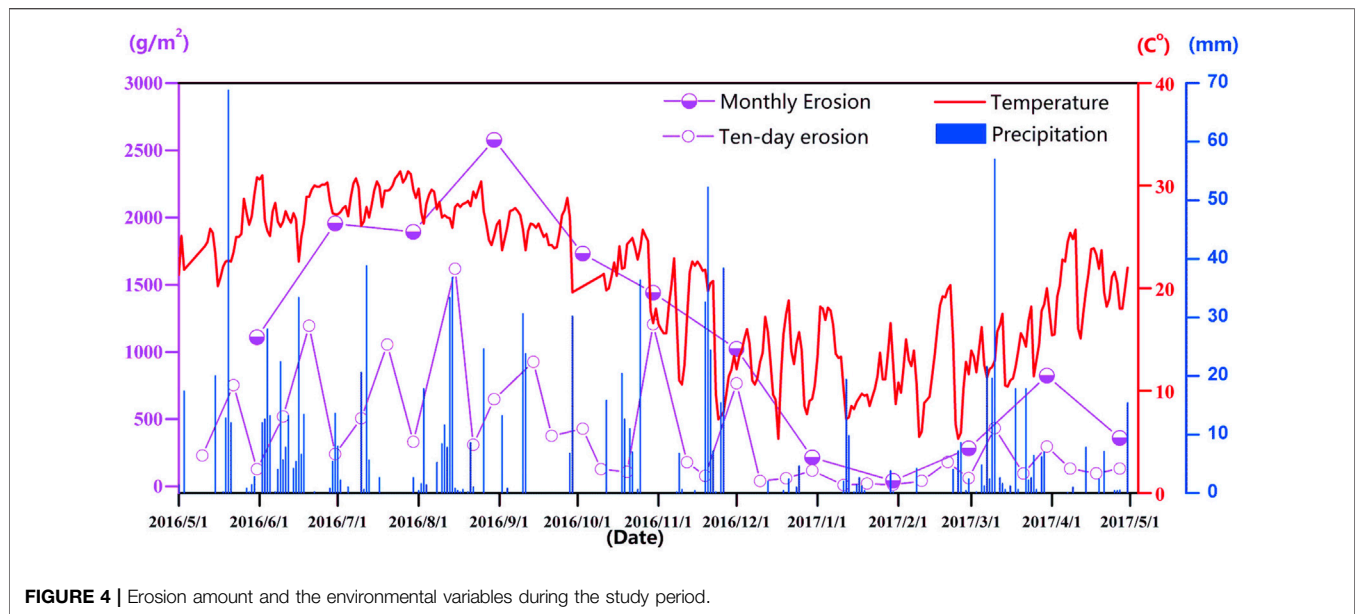


FIGURE 4 | Erosion amount and the environmental variables during the study period.

TABLE 2 | Erosion rates during study period.

Period	Mean temperature (°C)	Total precipitation (mm)	Erosive precipitation (mm)	Erosion rate (Mg ha ⁻¹ yr ⁻¹)
May 11, 2016–May 22, 2016	23.2	113.8	113	249.52
May 22, 2016–May 31, 2016	27.2	5.2	0	51.83
May 31, 2016–Jun 10, 2016	27.4	98	75	189.69
Jun 10, 2016–Jun 20, 2016	26.6	84	58	435.56
Jun 20, 2016–Jun 30, 2016	29.3	20	0	87.97
Jun 30, 2016–Jul 10, 2016	28.3	18	29.4	184.58
Jul 10, 2016–Jul 20, 2016	28.6	30	50	385.22
Jul 20, 2016–Jul 30, 2016	30.6	0	0	120.82
Jul 30, 2016–Aug 15, 2016	28.0	127.8	98	369.12
Aug 15, 2016–Aug 22, 2016	28.4	10	0	161.33
Aug 22, 2016–Aug 30, 2016	27.1	25.6	24.6	295.84
Aug 30, 2016–Sep 14, 2016	26.2	68.4	66	225.44
Sep 14, 2016–Sep 21, 2016	25.2	0	0	195.64
Sep 21, 2016–Oct 03, 2016	25.4	37	30	130.23
Oct 03, 2016–Oct 10, 2016	21.2	0	0	66.43
Oct 10, 2016–Oct 20, 2016	21.8	48.8	47	39.03
Oct 20, 2016–Oct 30, 2016	23	55	36	439.94
Oct 30, 2016–Nov 12, 2016	16.2	7.6	0	50.37
Nov 12, 2016–Nov 19, 2016	22.1	33	32.6	40.49
Nov 19, 2016–Dec 01, 2016	12.6	137.8	127	233.1
Dec 01, 2016–Dec 10, 2016	13.2	0	0	15.70
Dec 10, 2016–Dec 20, 2016	12.8	2.4	0	21.54
Dec 20, 2016–Dec 30, 2016	12.4	8	0	42.71
Dec 30, 2016–Jan 11, 2017	15	0	0	2.92
Jan 11, 2017–Jan 20, 2017	8.7	37	19	8.03
Jan 20, 2017–Jan 30, 2017	11.8	4	0	4.02
Jan 30, 2017–Feb 10, 2017	10.7	2.2	0	13.87
Feb 10, 2017–Feb 20, 2017	14.5	0	0	65.7
Feb 20, 2017–Feb 28, 2017	11	22.6	0	28.11
Feb 28, 2017–May 10, 2017	13	106.8	40	49.40
May 10, 2017–May 21, 2017	13.6	24.4	17.8	10.8
May 21, 2017–May 30, 2017	16	42.8	17.8	37.43
May 30, 2017–April 9, 2017	20.7	0.1	0	16.7
April 9, 2017–April 19, 2017	21.1	8.8	0	11.05
April 19, 2017–April 27, 2017	20.4	10.8	0	16.65
April 27, 2017–May 10, 2017	22.6	52	50	18.95
				4,315

TABLE 3 | Granger causality test results.

Dependent variable: TER (Ten-day erosion rate)			
Excluded	Chi-sq	df	Probability
TTP	4.978,858	1	0.0257
TMT	4.533,667	1	0.0332
All	7.262,643	2	0.0265

Note: *df* represents the degree of freedom; If probability is < 0.05, then a null hypothesis can be rejected, meaning that there is a causal relationship.

Granger causality tests are summarized in **Table 3**, which indicate variable causal links between erosion rates and TMT, erosion rates and TTP. Moreover, TTP and TMT were found to have positively contributed to increases in erosion rates ($p = 0.05$).

Impulse Response and Variance Decomposition

Impulse response analysis was deployed to analyze the dynamic relationship between erosion rate and environmental variables. As shown in **Figure 5**, providing a positive standard deviation shock is given to the residual of erosion rates, the rest of the variables react to this innovation. TTP response to erosion rates was found first to decrease, then fluctuate to become stationary in

the long-term. The response of TMT to erosion rates fluctuated at first and then stabilized due to shocks stemming from TER. Since the impulse response tends towards stability, the Granger causality tests are reasonable.

The variance decomposition approach was adapted to compare the contribution of rainfall and temperature to erosion rates. From No. Seven periods, the impulse response tended towards stability. Thus, the result of the impulse response was deemed to be reliable. Moreover, to forecast precipitation and temperature impacts on erosion rates, a variance decomposition and impulse response analyses were performed (**Table 4**). According to the variance decomposition analysis results presented in **Table 3**, 72.75% of the variation in erosion amounts could be attributed to innovative shocks within the variable itself. In comparison, the contribution made by TMT and TTP was 14.64 and 12.61%, respectively.

DISCUSSION

In some areas, frost action, snowmelt, and freeze-thaw processes are known to have important impacts on the weathering and erosion of badland surfaces (Regüés et al., 2000; Schumm, 1964; Regüés et al., 1995). In the Nanxiong Basin, with its subtropical climate, freezing occurs only a few times a year and it is not,

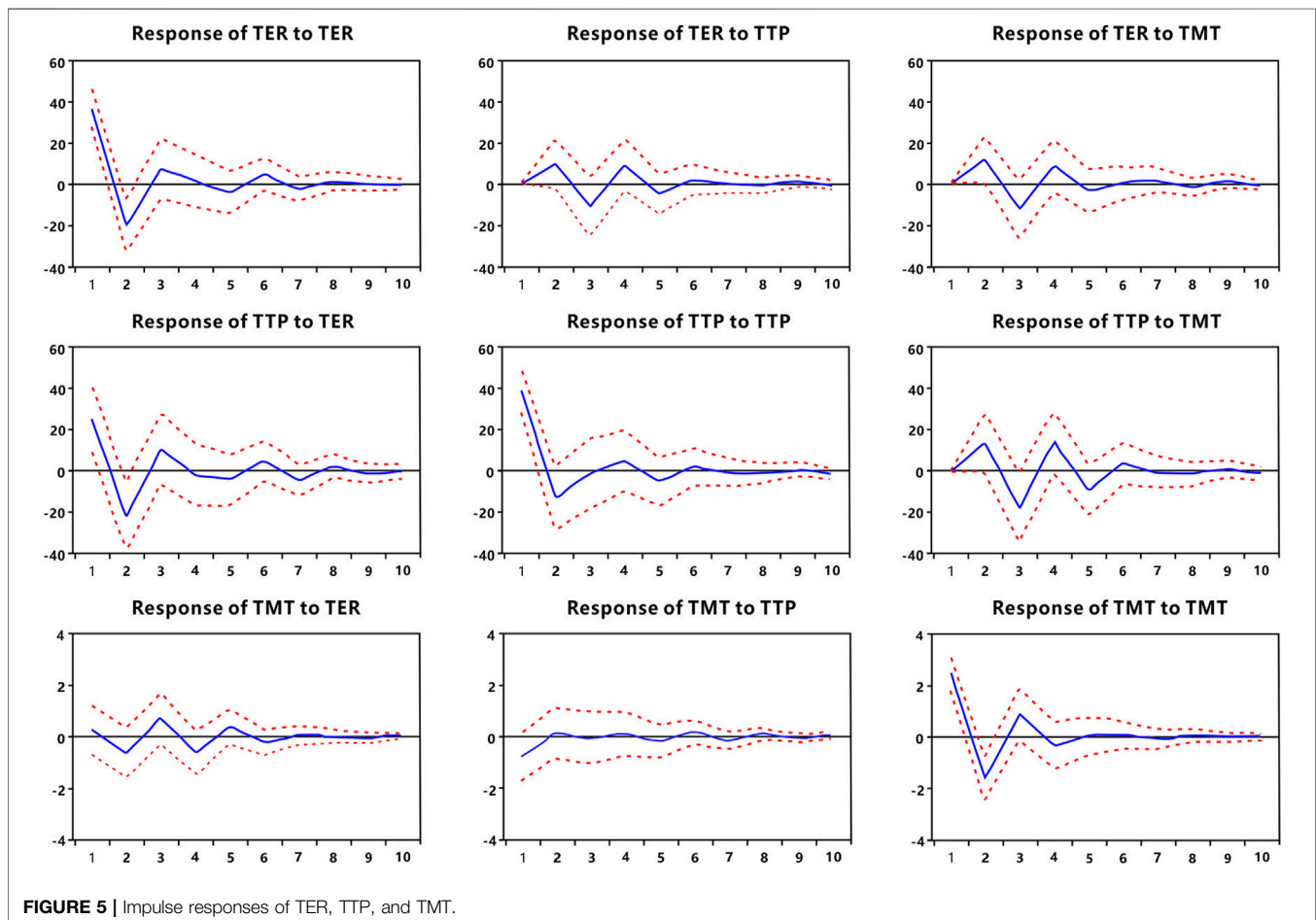
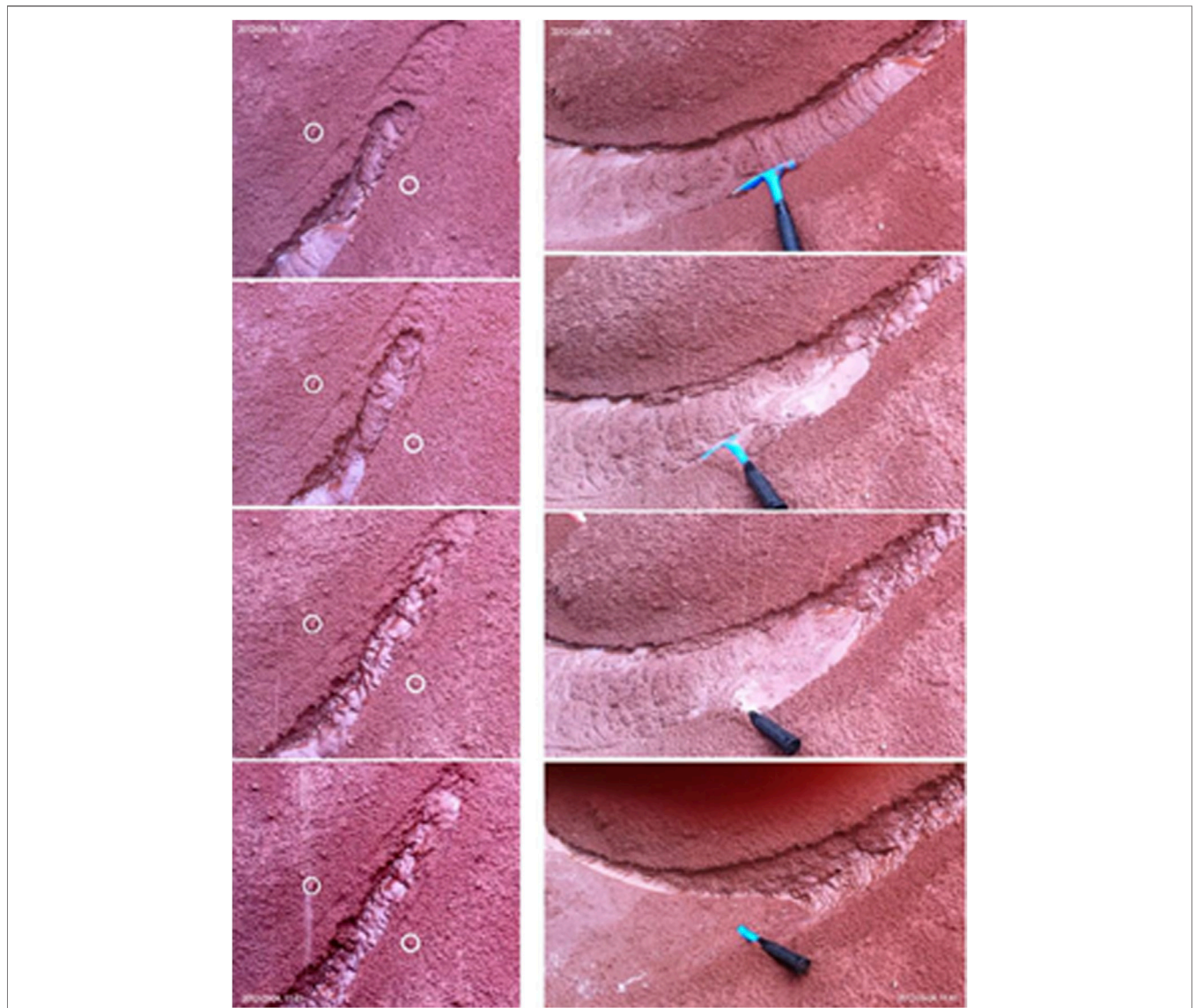


TABLE 4 | Variance Decomposition of TER (Ten-day erosion rate).

Standard error	TER	TTP	TMT
36.69031	100.0000	0.000000	0.000000
44.66480	88.87317	4.484,976	6.641,857
48.21860	78.38479	9.334,726	12.28048
49.73430	73.73669	11.89211	14.37119
50.30136	72.83393	12.60055	14.56552
50.51167	72.94112	12.61316	14.44572
50.60956	72.95709	12.56648	14.47643
50.66356	72.85255	12.57843	14.56903
50.69095	72.77387	12.60292	14.62321
50.70251	72.75058	12.61334	14.63608

therefore, considered to be a significant geomorphic factor. Excluding freezing processes, badland erosion occurs in response to individual rain events *via* rain-splash,

concentrated and unconcentrated surface flow, creep, mass movement, and piping (Bryan and Yair, 1982). Rain-splash and creep in particular shape the characteristic convexity of the upper slopes of badland landscapes (Parsons and Abrahams, 1994; Schumm, 1956; Carson and Kirkby, 1972). Surface runoff in the form of thin films is likely to be important for transporting material that has been detached and mobilized by splash and raindrop impact (Parsons and Abrahams, 1992; Abrahams et al., 1994). The effectiveness of creep and mudflow becomes apparent at high slope angles, where the thin weathered surface, once wetted, can begin to sag downslope under the influence of gravity (Clarke and Rendell, 2006). The impact of rain and mudflow was also notable at our study site, with mudflows appearing to transport most of the fragments from the slope face (**Figure 6**). A similar phenomenon is also recorded in Basilicata, Italy, where the effect of creep

**FIGURE 6** | Creep or mudflow occurs during continuous rain was observed during the monitoring period.

appears to be limited to a 10–40 mm thick weathered layer, where the sagging effect is visible on steep ($>53^\circ$) Biancane slopes (Clarke and Rendell, 2006). Thus, we speculate that the mudflows explain how TTP is related to removal fragments in Badlands in Nanxiong Basin. Further research is now required to determine the precipitation threshold for mudflow initiation.

Gravity has been identified as the primary morphogenic process responsible for shaping slopes in badlands (Ciccacci et al., 2008). In Nanxiong, small slides of dry fragments under a small perturbation are another notable form of erosion. During the periods when no erosive rain events occurred, such small-scale slides resulted in the highest erosion rate of $195.64 \text{ Mg ha}^{-1} \text{ yr}^{-1}$, which was almost 65 times higher than the lowest recorded erosion rate of $2.92 \text{ Mg ha}^{-1} \text{ yr}^{-1}$. Parsons and Abrahams (1994) note that the maximum slope angles of badland surfaces are related to the angle of repose of dry weathered detritus. In the Nanxiong badlands, slope angle equals the angle of frictional resistance, thus promoting the transport of weathered fragments downslope. The initiation of small dry slides involves disturbing animals, such as birds and insects, and wind.

Badlands developed in sub-humid mountainous areas are subject to higher rates of denudation and more active dynamics compared to similar landscapes in arid or semiarid areas (Bull and Kirkby, 2001; Regüés and Gallart, 2004).

Previous studies demonstrated that wetting and drying cycles are more effective at causing the disintegration of clay-bearing rocks (Erguler and Shakoor, 2009; Yan, et al., 2019). However, in the field, precipitation amounts recorded between sampling periods did not significantly correlate with rock bulk density or surface mechanical resistance, indicating that regolith moisture does not depend solely on precipitation at this site but also related to temperature (Nadal-Romero et al., 2007). Thus, we speculate that the mean temperature contributes to increase the number of wetting and drying cycles. This might explain why, at our study site, mean temperature was found to contribute 14.6% of erosion rates, which was slightly higher than the contribution of total precipitation (12.6%).

It is apparent that mean temperature (including the mean lowest and highest temperatures) had a stronger relationship with erosion rates over monthly timescale than temperature difference. However, over a ten-day timescale, while the correlation was significant, the M-K tau coefficient was low. Remarkably, the mean temperature was found to have casual links with erosion rates rather than temperature differences. High temperatures were also found to be dominant in increasing erosion rates. Thus, it appears that the coefficient of the ten-day temperature difference and erosion rates resulted from a time-lag effect of temperature. Work is now needed using long-term datasets to quantify the nature of this time interval.

In this climate and lithology, mean temperature rather than temperature difference has more of an influence on the erosion rates of badland slopes. As for other dry badlands, weathering dynamics depend mainly on rainfall characteristics and water deficit (Sole-Benet et al., 1997). For example, Gallart et al. (2002) reported that in the Vallcebre catchments of the Pyrenean ranges, the main controlling factor on badland development appears to be low

temperatures rather than a lack of moisture. Indeed, at our subtropical study site, the temperature was found to have at least the same influence as precipitation on the erosion of badland slopes.

We applied the Granger causality method to examine the relationships between climate variables and erosion rates over short temporal scales. In this sense, the dataset we need for this test is not necessarily from two or more years, although we are aware that more extended datasets have preferable. Nevertheless, the impulse response has shown that the result of the impulse response is reliable. Thus we believe that studies with only one are fine.

CONCLUSION

Analysis based on M-K τ correlation tests suggests that temperature variables positively and significantly correlated with erosion rates in the Nanxiong badlands. Granger causality relationships were also derived for erosion rates and TMT and total TTP. The results of impulse response and variance decomposition analyses show that the relative contributions of TMT and TTP to erosion were 14.6 and 12.61% during the study period, respectively. This suggests that in this subtropical environment, high mean temperatures have at least the same influence on badland development as precipitation. This implies that mean temperature might be an important parameter for erosion forecasting.

During the year-long study, 22.5% of the total erosion amount occurred during periods when no erosive rain events occurred. During these periods, small slides of dry weathered fragments were important for the removal of material in this transport-limited humid badland landscape, while mudflow processes were important for transporting material during periods of continuous rain.

DATA AVAILABILITY STATEMENT

The original contributions presented in the study are included in the article/Supplementary Material, further inquiries can be directed to the corresponding authors.

AUTHOR CONTRIBUTIONS

CZ and YL: Investigation, Data curation, Writing Original draft, Reviewing and Editing. CZ and PH: Conceptualization, Methodology, Supervision, Project administration, Funding acquisition. SH: Software, Validation, Visualization.

FUNDING

This study was funded by the National Natural Science Foundation of China (Grant No. 41901005) and Fundamental Research Funds for the Central Universities (SWU 118202). The corresponding author gratefully acknowledges financial support from China Scholarship Council (Grant No. CSC201806995083).

REFERENCES

- Abrahams, A. D., Howard, A. D., and Parsons, A. J. (1994). "Rock-Mantled Slopes," in *Geomorphology of Desert Environments* (London: Chapman and Hall), 173–212. doi:10.1007/978-94-015-8254-4_8
- Alexander, R. W., Calvo-Cases, A., Arnau-Rosalén, E., Mather, A. E., and Lázaro-Suau, R. (2008). Erosion and stabilisation sequences in relation to base level changes in the El Cautivo badlands, SE Spain. *Geomorphology* 100, 83–90. doi:10.1016/j.geomorph.2007.10.025
- Bocco, G. (1991). Gully erosion: Processes and models. *Prog. Phys. Geogr. Earth Environ.* 15, 392–406. doi:10.1177/030913339101500403
- Brandolini, P., Pepe, G., Capolongo, D., Cappadonia, C., Cevasco, A., Conoscenti, C., et al. (2017). Hillslope degradation in representative Italian areas: Just soil erosion risk or opportunity for development?. *Land Degrad. Dev.* 29, 3050–3068. doi:10.1002/ldr.2672
- Bryan, R. B., and Yair, A. (1982). *Badland Geomorphology and Piping*. Norwich: Geobooks, 407.
- Bull, N. J., and Kirkby, M. J. (2001). *Dryland Rivers: Processes and Management in Mediterranean Climates*. New Jersey, United States: Wiley.
- Campbell, I. A. (1997). "Badlands and Badland Gullies," in *Arid Zone Geomorphology: Process, Form and Change in Drylands*. Editor D. S. G. Thomas (London: Belhaven), 159–183.
- Campbell, I. A., and Honsaker, J. L. (1982). "Variability in Badlands Erosion; Problems of Scale and Threshold Identification," in *Space and Time in Geomorphology*. Editor C. E. Thorn (London: George Allen and Unwin.), 59–79.
- Cantón, Y., Solé-Benet, A., Queralt, I., and Pini, R. (2001). Weathering of a gypsum-calcareous mudstone under semi-arid environment at Tabernas, SE Spain: laboratory and field-based experimental approaches. *Catena* 44, 111–132. doi:10.1016/s0341-8162(00)00153-3
- Carson, M. A., and Kirkby, M. J. (1972). *Hillslope form and process*. UK: Cambridge University.
- Churchill, R. R. (1981). Aspect-Related Differences in Badlands Slope Morphology. *Ann. Assoc. Am. Geogr.* 71, 374–388. doi:10.1080/13520806.1981.11759448
- Ciccacci, S., Galiano, M., Roma, M. A., and Salvatore, M. C. (2008). Morphological analysis and erosion rate evaluation in badlands of Radicofani area (Southern Tuscany - Italy). *Catena* 74, 87–97. doi:10.1016/j.catena.2008.03.012
- Clarke, M. L., and Rendell, H. M. (2010). Climate-driven decrease in erosion in extant Mediterranean badlands. *Earth Surf. Process. Landforms* 35, 1281–1288. doi:10.1002/esp.1967
- Clarke, M. L., and Rendell, H. M. (2006). Process-form relationships in Southern Italian badlands: erosion rates and implications for landform evolution. *Earth Surf. Process. Landforms* 31, 15–29. doi:10.1002/esp.1226
- Desir, G., and Marín, C. (2009). Caracterización de la erosión en áreas acarcavadas en la Fm. Tudela (Bardenas Reales, Navarra). *Cuadernos de Investigación Geográfica* 35, 195–213. doi:10.18172/cig.1218
- Dickie, J. A., and Parsons, A. J. (2012). Eco-Geomorphological Processes within Grasslands, Shrublands and Badlands in the Semi-Arid Karoo, South Africa. *Land Degrad. Develop.* 23, 534–547. doi:10.1002/ldr.2170
- Dogan, E., and Aslan, A. (2017). Exploring the relationship among CO 2 emissions, real GDP, energy consumption and tourism in the EU and candidate countries: Evidence from panel models robust to heterogeneity and cross-sectional dependence. *Renew. Sust. Energ. Rev.* 77, 239–245. doi:10.1016/j.rser.2017.03.111
- Erguler, Z. A., and Shakoov, A. (2009). Relative contribution of various climatic processes in disintegration of clay-bearing rocks. *Eng. Geology*. 108, 36–42. doi:10.1016/j.enggeo.2009.06.002
- Fairbridge, R. W. (1968). *The Encyclopedia of Geomorphology*. New York: Reinhold, 1295.
- Gallart, F., Llorens, P., Latron, J., and Regúés, D. (2002). Hydrological processes and their seasonal controls in a small Mediterranean mountain catchment in the Pyrenees. *Hydrol. Earth Syst. Sci.* 6, 527–537. doi:10.5194/hess-6-527-2002
- Granger, C. W. J. (1969). Investigating causal relations by econometric models and cross-spectral methods. *Econometrica* 37, 424–438. doi:10.2307/1912791
- Granger, C. W. J. (1988). Some recent development in a concept of causality. *J. Econom.* 39, 199–211. doi:10.1016/0304-4076(88)90045-0
- Jiang, J., Wang, J., and Wei, X. (2015). Study on the Purple Soil Water Properties in Nanxiong City. *Chin. Agric. Sci. Bull.* 31, 215–218.
- Jiang, Z., and Li, X. (1988). Study on the Rainfall Erosivity and the Topographic Factor of Predicting Soil Loss Equation in the Loess Plateau. *Memoir Northwest. Inst. Soil Water Conservation Academia Sinica* 7, 40–45.
- Kasanin-Grubin, M., and Bryan, R. (2007). Lithological properties and weathering response on badland hillslopes. *Catena* 70, 68–78. doi:10.1016/j.catena.2006.08.001
- Ma, M., Liu, X., and Wang, W. (2018). Palaeoclimate evolution across the Cretaceous-Palaeogene boundary in the Nanxiong Basin (SE China) recorded by red strata and its correlation with marine records. *Clim. Past* 14, 287–302. doi:10.5194/cp-14-287-2018
- Martín-Moreno, C., Fidalgo Hijano, C., Martín Duque, J. F., González Martín, J. A., Zapico Alonso, I., and Laronne, J. B. (2014). The Ribagorda sand gully (east-central Spain): Sediment yield and human-induced origin. *Geomorphology* 224, 122–138. The Ribagorda sand gully (east-central Spain): Sediment yield and human-induced origin. doi:10.1016/j.geomorph.2014.07.013
- Martínezcasasnovas, J. A., Concepción Ramos, M., and García Hernández, D. (2010). Effects of land-use changes in vegetation cover and sidewall erosion in a gully head of the Penedès region (northeast Spain). *Earth Surf. Process. Landforms* 34, 1927–1937.
- Molina, A., Govers, G., Cisneros, F., and Vanacker, V. (2009). Vegetation and topographic controls on sediment deposition and storage on gully beds in a degraded mountain area. *Earth Surf. Process. Landforms* 34, 755–767. doi:10.1002/esp.1747
- Moreno-de las Heras, M., and Gallart, F. (2016). Lithology controls the regional distribution and morphological diversity of montane Mediterranean badlands in the upper Llobregat basin (eastern Pyrenees). *Geomorphology* 273, 107–115. doi:10.1016/j.geomorph.2016.08.004
- Nadal-Romero, E., Petrlík, K., Verachtert, E., Bochet, E., and Poesen, J. (2014). Effects of slope angle and aspect on plant cover and species richness in a humid Mediterranean badland. *Earth Surf. Process. Landforms* 39, 1705–1716. doi:10.1002/esp.3549
- Nadal-Romero, E., Regúés, D., Martí-Bono, C., and Serrano-Muela, P. (2007). Badland dynamics in the Central Pyrenees: Temporal and spatial patterns of weathering processes. *Earth Surf. Process. Landforms* 32, 888–904. doi:10.1002/esp.1458
- Parsons, A. J., and Abrahams, A. D. (1994). *Geomorphology of Desert Environments*. Netherlands: Springer.
- Parsons, A. J., and Abrahams, A. D. (1992). *Overland flow*. London: UCL Press, 307–334.
- Peng, H., Yan, L. B., Chen, Z., Scott, S., and Luo, G. S. (2015). A preliminary study of desertification in red beds in the humid region of Southern China. *ACTA GEOGRAPHICA SINICA* 70, 1699–1707.
- Regúés, D., and Gallart, F. (2004). Seasonal patterns of runoff and erosion responses to simulated rainfall in a badland area in Mediterranean mountain conditions (Vallcebre, southeastern Pyrenees). *Earth Surf. Process. Landforms* 29, 755–767. doi:10.1002/esp.1067
- Regúés, D., Guardia, R., and Gallart, F. (2000). Geomorphologic agents versus vegetation spreading as causes of badland occurrence in a Mediterranean subhumid mountainous area. *Catena* 40, 173–187. doi:10.1016/s0341-8162(99)00045-4
- Regúés, D., Pardini, G., and Gallart, F. (1995). Regolith behaviour and physical weathering of clayey mudrock as dependent on seasonal weather conditions in a badland area at Vallcebre, Eastern Pyrenees. *Catena* 25, 199–212. doi:10.1016/0341-8162(95)00010-p
- Schumm, S. A. (1964). Seasonal variations of erosion rates and processes on hillslopes in western Colorado. *Z. für Geomorphologie* 5, 215–238.
- Schumm, S. A. (1956). The role of creep and rainwash on the retreat of badland slopes [South Dakota]. *Am. J. Sci.* 254, 693–706. doi:10.2475/ajs.254.11.693
- Sole-Benet, A., Calvo, A., and Cerda, A. (1997). Influences of micro-relief patterns and plant cover on runoff related processes in badlands from Tabernas (SE Spain). *Catena* 31, 23–38.

- Wischmeier, W. H., and Smith, D. D. (1978). *USDA Agricultural Handbook*, 537.
- Yair, A., Bryan, R. B., Lavee, H., Schwanghart, W., and Kuhn, N. J. (2013). The resilience of a badland area to climate change in an arid environment. *Catena* 106, 12–21. doi:10.1016/j.catena.2012.04.006
- Yan, L., He, R., Kašanin-Grubin, M., Luo, G., Peng, H., and Qiu, J. (2017). The Dynamic Change of Vegetation Cover and Associated Driving Forces in Nanxiong Basin, China. *Sustainability* 9, 443. doi:10.3390/su9030443
- Yan, L., Liu, P., Peng, H., Kašanin-Grubin, M., and Lin, K. (2019). Laboratory study of the effect of temperature difference on the disintegration of redbed softrock. *Phys. Geogr.*, 1–15.

Conflict of Interest: The authors declare that the research was conducted in the absence of any commercial or financial relationships that could be construed as a potential conflict of interest.

Copyright © 2021 Chen, Yan, Peng and Shi. This is an open-access article distributed under the terms of the Creative Commons Attribution License (CC BY). The use, distribution or reproduction in other forums is permitted, provided the original author(s) and the copyright owner(s) are credited and that the original publication in this journal is cited, in accordance with accepted academic practice. No use, distribution or reproduction is permitted which does not comply with these terms.